Step-templated CVD growth of aligned graphene nanoribbons supported by a single-layer graphene film

Ago, Hiroki
Institute for Materials Chemistry and Engineering, Kyushu University | Graduate School of Engineering Sciences, Kyushu University

Ito, Yoshito
Graduate School of Engineering Sciences, Kyushu University

Tsuji, Masaharu
Institute for Materials Chemistry and Engineering, Kyushu University

Ikeda, Ken-ichi
Graduate School of Engineering Sciences, Kyushu University

出版情報：Nanoscale. 4 (16), pp.5178-5182, 2012-06-29. Royal Society of Chemistry
バージョン：

Step-templated CVD growth of aligned graphene nanoribbons supported by single-layer graphene film

Hiroki Ago,*[a,b] Yoshito Ito,[b] Masaharu Tsuji,[a] Ken-ichi Ikeda[b]

We present chemical vapor deposition (CVD) growth of a hybrid structure of aligned graphene nanoribbons (GNRs) supported by a single-layer graphene sheet. The step structure created on the epitaxial Co film is used to segregate arrays of aligned GNRs. Reflecting the highly ordered step structure of the Co catalyst, straight nanoribbons with high aspect ratio (>100) are formed. Analysis suggests that a large-area, single-layer graphene film also grows over the aligned GNRs, making a GNR-graphene hybrid structure. We also demonstrate the isolation of aligned GNRs by oxygen plasma treatment or partial transfer of the hybrid film. These findings on the formation of highly aligned GNRs give new insights on the formation mechanism of graphene and can be applied for more advanced graphene structure for future electronics.

Introduction

Graphene has attracted a great interest for the unique physical properties which are based on its ideal two dimensional structure as well as promising applications in many fields, such as flexible electronics and high-frequency devices.[1] The unique properties originate from the linear band dispersion crossing at the *K*-point, which makes single-layer graphene a zero-gap semiconductor. This zero-gap hinders the application of graphene to semiconductor applications, because it is difficult to obtain high on/off ratio in graphene transistors, although the carrier mobility is extremely high. There are two approaches to open the band gap. One is to apply a vertical electric field to double-layer graphene.[2] Another is to process a graphene sheet into stripes with nanoscale width, which are known as graphene nanoribbons (GNRs). In the GNRs, the band gap opening is theoretically expected due to quantum confinement in the one-dimensional nanostructure.[3,4] Several methods have been applied to synthesize GNRs, such as top-down lithography,[5,6] unzipping carbon nanotubes[7,8] and H_2 plasma etching.[9] These methods employ plasma or acid treatment which tends to damage the original graphene film. In addition, the edges of GNRs which strongly influence the electronic structure are usually difficult to be controlled.

Therefore, the bottom-up approach is useful for the preparation of defect-free graphene nanoribbons. Recently, polymerization on a metal substrate has been utilized to synthesize a one-dimensional graphene structure.[10] Considering the recent development of chemical vapor deposition (CVD) growth of graphene sheets,[11-14] it is attractive to directly grow GNRs on a metal catalyst film by CVD. However, there has been no report on the CVD growth of GNRs, to the best of our knowledge. This is because the planar metal film makes difficult to control the geometry of the segregated graphene film. Nanoscale metal patterns are not suitable for high temperature CVD process, because the high temperature distorts (or destroys) the fine metal pattern. Therefore, it is challenging to develop a direct CVD method to grow GNRs on metal films. In addition, it is interesting to integrate graphene with GNR for the improvement of electrical conduction while keeping the optical transparency.

Here, we demonstrate the direct CVD growth of GNRs on a heteroepitaxial Co thin film. Surface steps formed on the miscut sapphire substrate were used to create step structure on the heteroepitaxial Co film, which assists the graphene segregation along the Co steps. The GNRs are aligned normal to the miscut direction of sapphire and show very high aspect ratio (>100). The aligned GNRs are found to be covered with a single-layer graphene, and removal of the graphene film while leaving the aligned GNRs is also demonstrated.

Experimental

Figure 1 illustrates the experimental procedure. Sapphire c-plane substrates (α-Al_2O_3 (0001)) with intentional miscut, inclined to [1 $\bar{1}$ 2 0] direction with a miscut angle of 2.0º, were used. For comparison, we also studied low miscut angle (0.8º) substrates. These miscut substrates were purchased from Kyocera Co. Japan. The as-received sapphire substrates were first annealed in air at 900 ºC for 3 hours to create surface steps on the sapphire surface. Then, a 150 nm-thick Co film was epitaxially deposited by radio frequency (RF) sputtering at 500 ºC. Graphene was grown by ambient pressure CVD using a tubular furnace with a quartz tube with 26 mm inner diameter. The Co/sapphire substrate was placed in a quartz tube and annealed in H_2/Ar flow at 500 ºC for 3 hours, followed by elevating the temperature to 1000 ºC in Ar

flow. After reaching 1000 ºC, CH_4/H_2/Ar mixed gas (2/100/400 sccm, respectively) was flowed for 10 min. Then, the sample was cooled down to room temperature in H_2 gas flow.

Surface structures of sapphire and Co metals were examined by atomic force microscope (AFM, Bruker Nanoscope IIIa). As-grown graphene film was transferred to a target SiO_2 (300 nm)/Si substrate by using polymethyl methacrylate (PMMA), thermal tape, and etching solution (aqueous 1 M $FeCl_3$ solution). Details of the graphene transfer process are described elsewhere.[14-16] The transferred graphene was analyzed by optical microscope, scanning electron microscope (SEM, HITACHI S-4800) and Raman microscope (Tokyo Instruments, Nanofinder30). For cross-sectional observation of the graphene grown on Co film, transmission electron microscope (TEM, HITACHI H-9500) was used for a specimen cut by focused-ion beam (FIB, HITACHI NB5000). O_2 plasma treatment was performed with a plasma reactor (Yamato PR-500) with 300 W for 1 min.

Results and discussion

Shown in Fig. 2a is the AFM image of the thermally annealed sapphire surface with 2.0º miscut. We observed clear step/terrace structure whose orientation is normal to the miscut direction. The AFM height analysis indicates that the step height is 0.2-0.3 nm, which agrees with that of the single atomic step reported for c-plane sapphire (0.21 nm).[17] Due to the relatively high miscut angle, the terrace width was relatively narrow (5-20 nm). The AFM image of sapphire surface with low miscut angle, 0.8º, is also shown in Supplemental Information (Fig. S1a). After Co sputtering, the surface of the Co film was very smooth without clear step/terrace structure, as seen in Fig. 2b. The surface roughness measured by AFM (root mean square (rms)), of the Co surface was only 0.14 nm. However, after H_2 annealing followed by the reaction with CH_4, new step/terrace structure appeared on the Co surface (Fig. 2c,d) whose orientation is identical to the original step/terrace direction of the underneath sapphire. The surface structure of the Co strongly depends on the annealing process. As shown in Fig. S2, the CVD growth without H_2 annealing induced the formation of a number of pits on the Co surface and no clear step/terrace structure was seen on the Co surface. The successive H_2 annealing process at 500 ºC and 1000 ºC was found to be effective to obtain a clear step/terrace structure on the Co. On the other hand, too long H_2 annealing at 1000 ºC disturbed the sharp steps (see Fig. S2). We previously reported that the high temperature sputtering and successive H_2 annealing process significantly improve the crystallinity of Co metal, making single crystalline Co on sapphire.[14] Thus, the H_2 annealing is supposed to increase the crystallinity of the Co film which accompanies the reconstruction of the Co surface. The step height and terrace width differ from those of the original sapphire surface; the newly appeared structure on the Co surface had two different steps; dense steps with the low step height, <10 nm (Fig. 2c), and sparse steps with high step height, 20-40 nm (Fig. 2d). However, since the direction of the step structure is identical to that of the sapphire substrate, we consider that the surface morphology of the sapphire leads to the observed unique stepped structure on the Co surface.

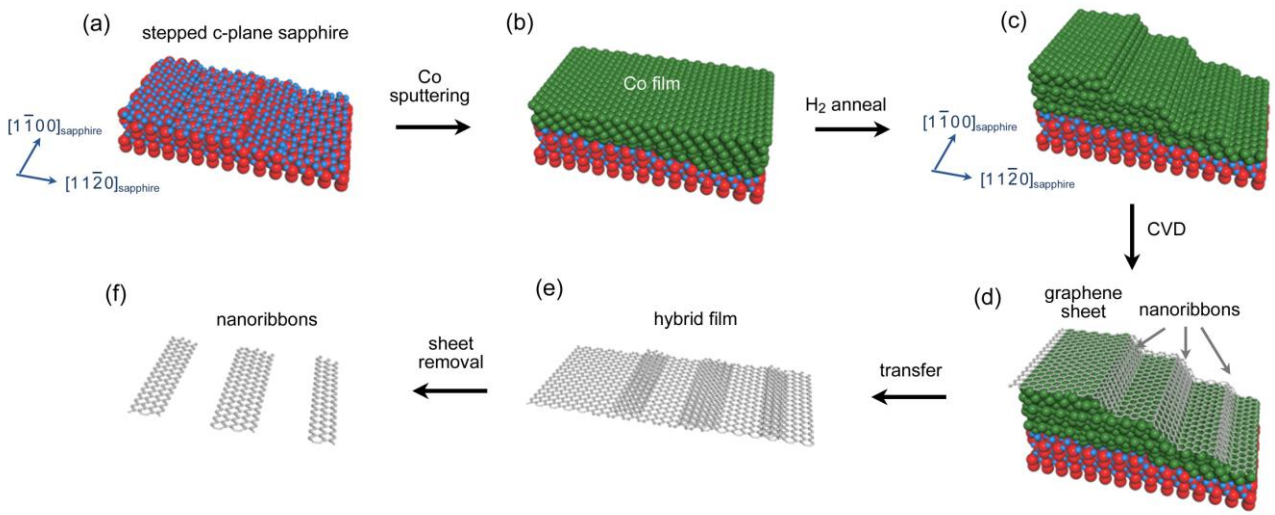

Figure 1 Schematic procedure of CVD growth of graphene-nanoribbon hybrid film and isolated graphene nanoribbon arrays. (a) Miscut sapphire c-plane substrate is annealed in air to make step/terrace structure. (b) Thin Co film is deposited on the sapphire while heating the substrate at 500 ºC. (c) The Co film is annealed in H_2 at 500 ºC and 1000 ºC to form the surface steps on the Co surface. (d) Graphene is grown on the Co film by introducing CH_4/H_2/Ar gas, followed by rapid cooling. After transfer (e), O_2 plasma treatment removes the graphene sheet, resulting in isolated GNRs (f).

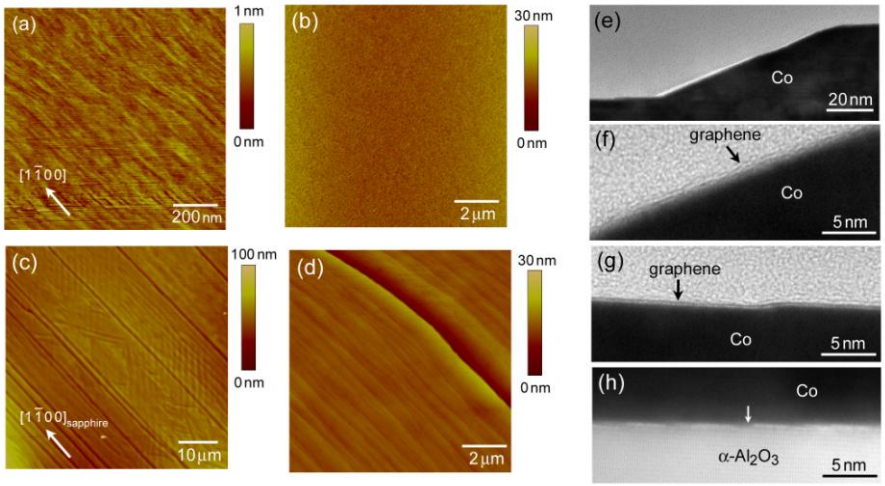

Figure 2 AFM images of the miscut sapphire surface after annealing in air (a), sputtered Co surface (b), and the Co surface after CVD (c,d). Miscut angle of sapphire is 2.0º. (e-h) Cross- sectional TEM images. (e) The high step, (f) step edge, (g) flat surface with low step, and (h) interface between Co and sapphire. The arrow in (h) indicates the surface atomic step of sapphire.

We investigated the cross-sectional TEM of the as-grown graphene sample. The specimen was cut from Co/sapphire by using a FIB and mounted on a TEM grid. Figure 2e shows the low magnification TEM image of a high step with 30 nm height. At the step surface, few layer graphene was seen (Fig. 2f), while single-layer graphene was mostly observed at the flat surface with low steps (Fig. 2g). Figure 2h shows the Co-sapphire interface where sapphire's atomic steps are clearly observed.

To further characterize the graphene grown on the Co surface, we transferred graphene from the Co film onto a target SiO_2/Si substrate using PMMA and $FeCl_3$ etching solution.[14-16] Optical microscope and SEM images of the transferred films are displayed in Fig. 3a-c. The transferred film showed linear dark optical contrasts running parallel to the [1100] direction of the sapphire substrate (Fig. 3a). These dark lines correspond to GNRs, as described later. One can see that the GNRs are very

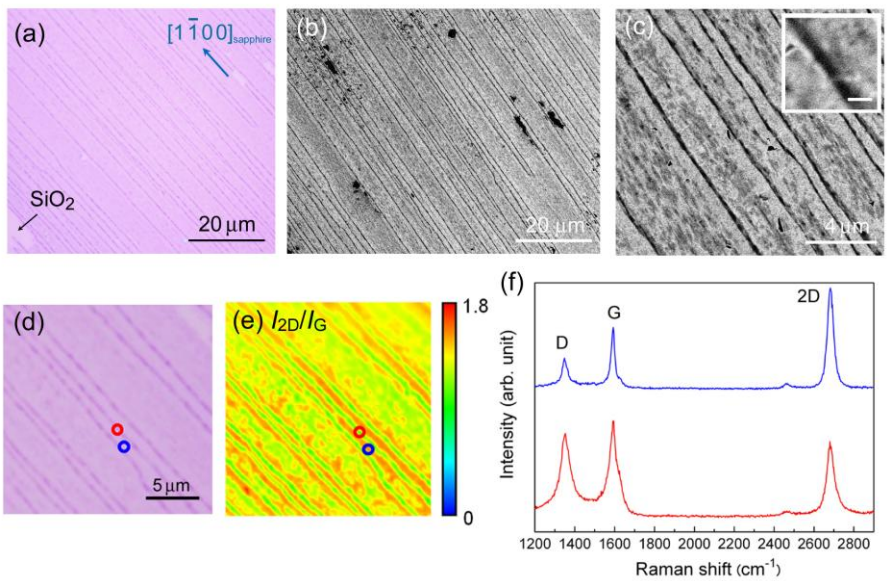

Figure 3 Optical microscope (a) and SEM (b,c) images of a transferred graphene-nanoribbon hybrid film. In (a), the exposed surface of SiO_2 substrate is indicated by an arrow. Scale bar of (c) inset is 200 nm. (d) Optical micrograph where Raman mapping is performed. The relative intensity of Raman 2D-band to G-band is mapped in (e). (f) Raman spectra measured at two points marked in (d,e). Red circle indicates the place where a GNR is present, while blue circle shows the place where no GNR is observed. The blue spectrum indicates that the graphene film is single-layer. Insets of (b,e) show the optical micrograph (scale bar: 4 μm)

straight and have a high aspect ratio exceeding 100. The direction of the aligned GNRs is uniform in the whole substrate surface, indicating that the step/terrace structure of the original sapphire substrate stimulates the growth of aligned GNRs.

From the angle measured by the cross-sectional TEM images (Fig. 2e,f), the step edge is determined to be (1 1 $\bar{2}$ 8) considering hcp(0001) surface for the Co film (see Fig. S3). In the case of Cu metal, the growth rate of graphene is reported to be dependent on the crystalline plane of Cu.[18] Thus, the, (1 1 $\bar{2}$ 8) plane, may assist the preferential segregation of graphene. On the other hand, there is another possibility that the corner of the step edge acts as the nucleation site, being similar to the case of grain boundaries in catalyst metal. The grain boundaries are known to promote the nucleation of graphene.[19] Therefore, the corner of our step edges may contribute to the formation of GNRs.

In Fig. 3a, bare SiO_2 surface is also seen as bright contrast (indicated by an arrow). From the optical contrast, we found that large single-layer graphene is grown together with the GNRs. The single-layer graphene covers more than half of the Co surface and the aligned GNRs are always observed together with this graphene sheet. We previously observed the uniform growth of single-layer graphene over heteroepitaxial Co film deposited on sapphire c-plane.[14] Thus, the segregation (or precipitation) of a graphene sheet is likely to occur simultaneously with the site-selective segregation at the high steps of the Co film.

Shown in Fig. 3b,c are SEM images of the transferred film. The contrast reflects the thickness of graphene layer and the darker contrast corresponds to thicker area. These SEM images also support the growth of an aligned GNRs-graphene hybrid structure. Based on the SEM observation, the GNRs are found to have widths of 200-800 nm. It is noted that the density of GNRs is almost comparable to that of the high steps seen in Fig. 2c, signifying the preferential segregation at the sparse high steps. The single-layer graphene film is not so uniform when compared in the SEM contrast. This may have originated from the non-uniform segregation at low steps and/or surface contamination with PMMA residue.

The Co film deposited on the sapphire with a low miscut angle, 0.8º, also catalyzed the growth of GNRs-graphene hybrid, as shown in Fig. S1c. However, the GNRs were wavy and the density was lower than that of high miscut angle sapphire. This is consistent with the AFM image of the Co surface after the CVD which showed a distorted step/terrace structure (Fig. S1b). This fact also implies that the step structure appeared on the Co film is strongly dependent on the sapphire surface.

Raman spectroscopy is a powerful tool for analyzing structure and layer numbers of graphene. We measured Raman spectra for the transferred film. The optical microscope image and the corresponding Raman mapping images are shown in Fig. 3d,e. The Raman spectra measured at the marked points are shown in Fig. 3f. The uniform film which covered the whole observed area (marked as the blue circles) showed the characteristic Raman spectrum of single-layer graphene; the high I_{2D}/I_G ratio ~1.5, narrow 2D band width (33 cm^{-1}) and 2D position (2680 cm^{-1}).[20,21] However, at different position of the sheet, the graphene film showed relatively low I_{2D}/I_G ratio ~1 probably due to non-uniform segregation at the low steps. The Raman spectrum measured at the point where a GNR is present (marked as red circle) showed the low I_{2D}/I_G ~0.8, signifying double- or multi-layer graphene (Fig. 3f). The 2D band is located at 2680 cm^{-1}

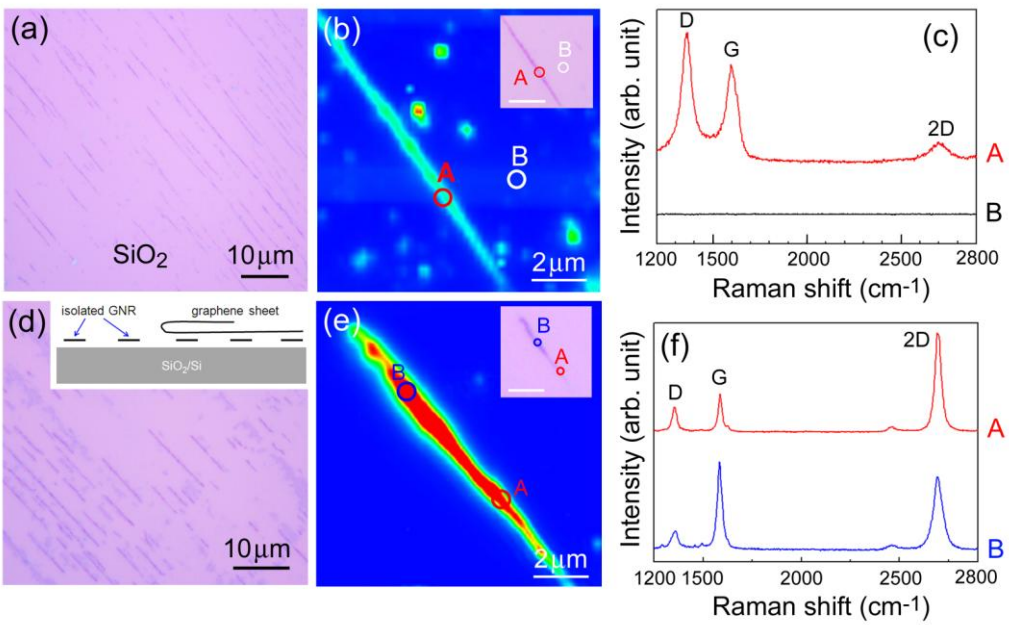

Figure 4 Isolated GNRs prepared by O_2 plasma etching (a-c) and removal of the first layer during transfer (d-f). (a,d) Optical micrographs, (b,e) Raman mapping images of 2D-band intensity, and (c,f) Raman spectra measured at the points marked in (b,e). Insets of (b,e) show the optical micrograph (scale bar: 4 μm). Inset of (d) illustrates the partial transfer of graphene nanoribbons observed after the transfer to SiO_2/Si wafer.

and the 2D band width is 40 cm^{-1}. Considering the presence of the single-layer graphene covering the GNRs, it is likely that the GNRs are either single- or few-layer. The D-band which is associated with domain boundary and structural defects are significantly enhanced at the GNR position. Since the spot size of our confocal Raman is ~600 nm, we consider that the GNR edges contribute the enhanced D-band.

When the carbon supply was reduced by lowering CH_4 concentration, the segregated area became smaller, but the single-layer graphene was always formed together with GNRs. It is known that graphene segregation or precipitation occurs at grain boundaries or pits of catalyst metal.[22,23] In particular, in a metal film with high carbon solubility (like Ni and Co), the dissolved carbon atoms are facile to diffuse widely in the metal film and precipitate during the cooling process. The high steps can act as such nucleation sites and forms GNRs along the steps. The importance of the cooling rate was also observed in our system,[24] and rapid cooling was essential to obtain the clear GNR-graphene hybrid structure. Furthermore, we found that the gas during the cooling process is important and pure H_2 gas is preferable for the clean segregation. When Ar gas with low concentration H_2 gas (H_2 4%) was used during the cooling process, thick graphene films were partly formed instead of uniformed single-layer graphene (Supplemental Information, Fig. S4).

It is interesting to study a sputtered Cu film as a catalyst, since single-layer graphene can be selectively grown on the Cu film.[12,15,16] However, due to low melting temperature of Cu (1083 ºC), no clear step/terrace structure was obtained on the Cu surface, as shown in Supplemental Information (Fig. S5). Even at 900 ºC, periodic step structure was not observed for the Cu film.

For electronic applications, it is necessary to remove a single-layer graphene sheet which covers the nanoribbons to obtain the isolated GNR array. Figure 4 presents our two approaches of removing the single-layer graphene for the isolation of GNRs. We applied O_2 plasma treatment for the GNR-graphene hybrid film. The resulting optical microscope image and Raman data are presented in Fig. 4a-c. The etching of single-layer graphene was confirmed by both optical microscope and Raman spectrum; no Raman signal was observed except for the remaining nanoribbons. The O_2 plasma treatment, however, damaged the remaining GNRs, as was seen by increased D-band and weakened 2D-band (Fig. 4c).

We occasionally observed the partial removal of single-layer graphene sheet, as shown in Fig. 4d. In the graphene transfer process, the single-layer graphene can be removed while leaving some of the GNRs attached to the Si surface (Fig. 4d inset). This result strongly suggests that the single-layer graphene sheet forms on top of GNRs. In the remaining GNR shown in Fig. 4e, the thickness is not uniform ranging from single- to few-layer, but it shows a moderate D-band and intense 2D-band (Fig. 4e,f), indicating higher quality than that produced by the O_2 plasma treatment (see Fig. 4c).

The selective removal of single-layer graphene sheet which covers the aligned GNRs needs further study. For example, the metal-assisted layer-layer removal of graphene recently reported by Dimiev et al.[25] might be applied to our hybrid structure. The GNR width should be reduced for opening the band gap. We need further study, such as using higher miscut angle sapphire and/or further optimization of the annealing condition, for the narrowing of the GNR width, because the surface structure of the Co metal plays an important role in the aligned GNR arrays.

However, we emphasize that this is the first demonstration of the direct CVD growth of GNR structure on metal film without employing any lithographic approach. Our finding can be developed to the direct CVD growth of highly-aligned GNR array which is applicable to semiconductor devices.

Conclusions

We demonstrate the direct CVD growth of GNR-single-layer graphene hybrid structure on the stepped Co surface. The step structure is created on an epitaxial Co film which is deposited on miscut sapphire substrate, and this structure realizes the graphene nucleation along the steps. The width of the aligned GNRs is 200-800 nm and the aspect ratio is higher than 100. The transferred film indicates that co-growth of single-layer graphene occurs together with the aligned GNRs. Two approaches to remove single-layer graphene sheet while retaining the GNRs are presented. The demonstration of growth at the step edge highlights the growth mechanism of CVD graphene and also offers a new route to fabricate GNR-based nanostructures with controlled orientation and density for future electronics applications.

Acknowledgements

This work is supported by JSPS Funding Program for Next Generation World-Leading Researchers (NEXT Program, #GR075).

Notes

[a] *Institute for Materials Chemistry and Engineering, Kyushu University Kasuga, Fukuoka 816-8580 (Japan); E-mail: ago@cm.kyushu-u.ac.jp*
[b] *Graduate School of Engineering Sciences, Kyushu University Kasuga, Fukuoka 816-8580 (Japan)*

† Electronic Supplementary Information (ESI) available: [details of any supplementary information available should be included here]. See DOI: 10.1039/b000000x/

References

1 A. K. Geim and K. S. Novoselov, *Nat. Mater.*, 2007, **6**, 183.
2 Y. Zhang, T. T. Tang, C. Girit, Z. Hao, M. C. Martin, A. Zettl, M. F. Crommie, Y. R. Shen and F. Wang, *Nature*, 2009, **459**, 820.
3 K. Tanaka, S. Yamashita, H. Yamabe and T. Yamabe, *Synth. Met.*, 1987, **17**, 143.
4 K. Nakada, D. Fujita, G. Dresselhaus and M. S. Dresselhaus, *Phys. Rev. B*, 1996, **54**, 17954.
5 M. Y. Han, J. C. Brant and P. Kim, *Phys. Rev. Lett.*, 2010, **104**, 56801.
6 J. Bai, X. Duan and Y. Huang, *Nano Lett.*, 2009, **9**, 2083.
7 L. Jiao, L. Zhang, X. Wang, G. Diankov and H. Dai, *Nature*, 2009, **458**, 877.
8 D. V. Kosynkin, A. L. Higginbotham, A. Sinitskii, J. R. Lomeda, A. Dimiev, B. K. Price and J. M. Tour, *Nature*, 2009, **458**, 872.

9 R. Yang, L. Zhang, Y. Wang , Z. Shi, D. Shi, H. Gao, E. Wang and G. Zhang, *Adv. Mater.*, 2010, **22**, 4014.
10 J. Cai, P. Ruffieux, R. Jaafar, M. Bieri, T. Braun, S. Blankenburg, M. Muoth, A. P. Seitsonen, M. Saleh, X. Feng, K. Müllen and R. Fasel, *Nature*, 2010, **466**, 470.
11 A. Reina, X. Jia, J. Ho, D. Nezich, H. Son, V. Bulovic, M. S. Dresselhaus and J. Kong, *Nano Lett.*, 2009, **9**, 30.
12 X. Li, W. Cai, J. An, S. Kim, J. Nah, D. Yang, R. Piner, A. Velamakanni, I. Jung, E. Tutuc, S. K. Banerjee, L. Colombo and R. S. Ruoff, *Science*, 2009, **324**, 1312.
13 S. Bae, H. Kim, Y. Lee, X. Xu, J. S. Park, Y. Zheng, J. Balakrishnan, T. Lei, H. R. Kim, Y. I. Song, Y. J. Kim, K. S. Kim, B. Özyilmaz, J. H. Ahn, B. H. Hong and S. Iijima, *Nat. Nanotech.*, 2010, **5**, 574.
14 H. Ago, Y. Ito, N. Mizuta, K. Yoshida, B. Hu, C. M. Orofeo, M. Tsuji, K. Ikeda and S. Mizuno, *ACS Nano*, 2010, **4**, 7407.
15 Y. Ogawa, B. Hu, C. M. Orofeo, M. Tsuji, K. Ikeda, S. Mizuno, H. Hibino and H. Ago, *J. Phys. Chem. Lett.*, 2012, **3**, 219.
16 B. Hu, H. Ago, Y. Ito, K. Kawahara, M. Tsuji, E. Magome, K. Sumitani, N. Mizuta, K. Ikeda and S. Mizuno, *Carbon*, 2012, **50**, 57.
17 M. Yoshimoto, T. Maeda, T. Ohnishi, H. Koinuma, O. Ishiyama, M. Shinohara, M. Kubo, R. Miura and A. Miyamoto, *Appl. Phys. Lett.*, 1995, **67**, 2615.
18 J. D. Wood, S. W. Schmucker, A. S. Lyons, E. Pop, J. W. Lyding, *Nano Lett.*, 2011, **11**, 4547.
19 Y. Zhang, L. Gomez, F. N. Ishikawa, A. Madaria, K. Ryu, C. Wang, A. Badmaev, C. Zhou, *J. Phys. Chem. Lett.*, 2010, **1**, 3101.
20 A. C. Ferrari, J. C. Meyer, V. Scardaci, C. Casiraghi, M. Lazzeri, F. Mauri, S. Piscanec, D. Jiang, K. S. Novoselov, S. Roth and A. K. Geim, *Phys. Rev. Lett.*, 2007, **97**, 187401.
21 C. M. Orofeo, H. Ago, B. Hu and M. Tsuji, *Nano Res.*, 2011, **4**, 531.
22 G. H. Han, F. Güneş, J. J. Bae, E. S. Kim, S. J. Chae, H.-J. Shin, J.-Y. Choi, D. Pribat and Y. H. Lee, *Nano Lett.*, 2011, **11**, 4144.
23 H. Ago, I. Tanaka, C. M. Orofeo, M. Tsuji and K. Ikeda, *Small*, 2010, **6**, 1126.
24 A. Reina, S. Thiele, X. Jia, S. Bhaviripudi, M. S. Dresselhaus, J. A. Schaefer and J. Kong, *Nano Res.*, 2009, **2**, 509.
25 A. Dimiev, D. V. Kosynkin, A. Sinitskii, A. Slesarev, Z. Sun, J. M. Tour, *Science*, 2011, **331**, 1168.

Table of Contents

Hybrid structure of highly aligned graphene nanoribbons and a single-layer graphene sheet is realized on a stepped Co film.